



Communication

Preparation of mesoporous silica nanoparticle with tunable pore diameters for encapsulating and slowly releasing eugenol

Tianlu Zhang^{a,c,1}, Zhiguo Lu^{a,c,1}, Jianze Wang^a, Jie Shen^{a,c}, Qiulian Hao^a, Yan Li^{a,c}, Jun Yang^{a,c}, Yunwei Niu^{d,e}, Zuobing Xiao^{d,e}, Lei Chen^{b,**}, Xin Zhang^{a,c,*}

^a State Key Laboratory of Biochemical Engineering, Institute of Process Engineering, Chinese Academy of Sciences, Beijing 100190, China

^b Department of Obstetrics and Gynecology, Navy General Hospital of People Liberation Army, Beijing 100048, China

^c School of Chemical Engineering, University of Chinese Academy of Sciences, Beijing 100049, China

^d Shanghai Research Institute of Fragrance and Flavor Industry, Shanghai 200232, China

^e School of Perfume and Aroma Technology, Shanghai Institute of Technology, Shanghai 200233, China

ARTICLE INFO

Article history:

Received 13 October 2020

Received in revised form 16 December 2020

Accepted 17 December 2020

Available online 3 March 2021

Keywords:

Eugenol

Mesoporous silica nanoparticles

Nano-fragrance

Slow release of fragrance

ABSTRACT

Fragrances are frequently added to a variety of products, including food, cosmetics and health products. However, the high volatility and instability of essence limit its application in some fields. In this study, mesoporous silica nanoparticles (MSNs) were prepared to encapsulate eugenol, which could reduce the volatilization of the fragrance molecules. A facile approach was presented to synthesize MSNs with three different pore diameters for encapsulating eugenol. In addition, the properties of MSNs including mean particle size, morphology, encapsulating efficiency and release tendency were characterized. Results showed that the larger the pore diameters of MSNs, the more aromatic molecules were adsorbed. Furthermore, the release mechanism was described as the smaller the pore diameters of MSNs, the slower the release of eugenol.

© 2021 Chinese Chemical Society and Institute of Materia Medica, Chinese Academy of Medical Sciences. Published by Elsevier B.V. All rights reserved.

Fragrances have been applied widely in food, daily chemical, clothing and medicine industries, which can beautify people's lives [1–4]. However, most fragrance molecules are unstable [5,6]. During storage and production, their sensitive or volatile aromatic components are easy to deteriorate and lose [7,8]. Therefore, the key to improving the effect of fragrances and prolonging the service life of fragrant products is to design and prepare materials capable of slow-release the molecules.

Controlled release of aromatic molecules has always been a research hotspot in fragrance industry. With the developments of nanoscience and nanotechnology, many kinds of nanomaterials have been used to load and slowly release fragrance molecules, and the diffusion of the fragrance molecules is controlled by entrapping them into carriers. For example, cationic nanomaterials can adsorb anionic molecules through electrostatic interaction [9–12]. Some

carriers can covalently bind molecules to load molecules through chemical bonds [13–17]. Small molecules are encapsulated into nanoparticles such as micelles and liposomes, in order to realize the slow release of molecules [18–21]. A large number of methods have been reported to improve the slow release of fragrance, achieve stability, and realize durability of fragrance. However, different fragrances have different appropriate release rates. In addition, different people have different preferences for aroma concentration. The fragrance release rates of most nano-fragrances are untunable. Aromatic products are in great demand and the price is relatively low. Considering the industrial requirements of aromatic products, the preparation process of fragrance-loaded nanomaterials should be simple. However, it is difficult for most nanomaterials to realize low-cost and large-scale industrial production.

Mesoporous silica nanoparticles (MSNs) have strong adsorption capacity for volatile molecules due to their large specific surface area and pore volume [22–28]. Besides, it is expected that the encapsulation and release characteristics of fragrance molecules can be changed by adjusting the mesopores of MSNs. Therefore, MSNs are suitable for encapsulating and slowly releasing fragrance molecules. In addition, mesoporous silica nanoparticles have simple preparation and low production costs. Therefore, MSNs is

* Corresponding author at: State Key Laboratory of Biochemical Engineering, Institute of Process Engineering, Chinese Academy of Sciences, Beijing 100190, China.

** Corresponding author.

E-mail addresses: chenleis@mail.tsinghua.edu.cn (L. Chen), xzhang@ipe.ac.cn (X. Zhang).

¹ These authors contributed equally to this work.

suitable for loading perfume molecules and large-scale industrial production.

In this study, MSNs with tunable pore diameters were synthesized to load eugenol and the fragrance-loaded MSNs were named eugenol@MSNs. Eugenol is a perfume molecule with obvious scent of clove. It can be used for resisting bacteria and lowering blood pressure, and can also be used for preparing essence of cosmetics and daily chemical products [29,30]. In addition, studies have shown that eugenol also has the effect of regulating the central nervous system [31]. By changing the amount of *n*-hexane, different pore diameters were obtained. Subsequently, the effect of pore size on encapsulation and release of fragrance molecules was further explored (Scheme 1).

MSNs were prepared firstly. Tetraethyl orthosilicate (TEOS, 98%), hexadecyltrimethylammonium bromide (CTAB, 99%), *n*-hexane and eugenol (98%) were obtained from J&K Scientific. Ammonium hydroxide (28%) and ethanol (99%) were purchased from Sinopharm Chemical Reagent Co., Ltd. All other chemicals such as ethanol were obtained locally.

1.0 g of CTAB was dissolved in 160 mL of deionized water. 7 mL of ammonium hydroxide was then added into CTAB solution under stirring for 30 min. Then, different volumes of *n*-hexane were mixed with 5 mL TEOS, and then slowly added to the above solution drop by drop (finished within 30 min) at 35 °C for 12 h under stirring. The white precipitate (MSNs) was then collected by filtration under reduced pressure.

The morphologies of MSNs were observed using scanning electron microscope (SEM). The inner structures of MSNs were observed using transmission electron microscopy (TEM, JEOL 2100F). Then, the specific surface areas, pore size and pore volume of MSNs were measured and calculated by the Brunauer-Emmett-Teller (BET) method. Before measurement, the samples were degassed in vacuum at 180 °C for at least 6 h.

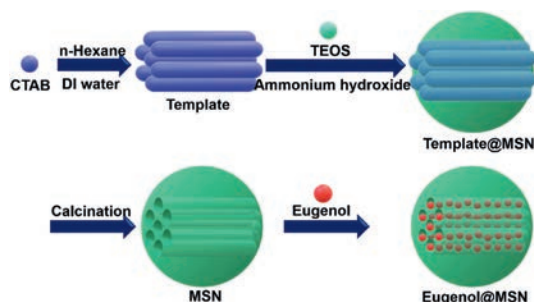
The obtained MSNs (100 mg) were dispersed into eugenol (10 mL) under vigorous stirring for 24 h. The unloaded eugenol was then removed by filtration under reduced pressure to obtain eugenol@MSNs.

Thermogravimetric analysis (TGA) was used to determine the thermostability of the fragrance and calculated the encapsulation efficiency of eugenol. This experiment was performed in the temperature from 25 °C to 600 °C at a heating rate of 10 °C/min under a constant nitrogen flow (20 mL/min). The encapsulation efficiency (*f*) was obtained according to formula (1):

$$\frac{W_1}{100 - f} = \frac{W_2}{100 - W_2} \quad (1)$$

where W_1 is the weight loss of the eugenol@MSNs and W_2 is the weight loss of the MSNs.

Then, the eugenol (20 mg) and eugenol@MSNs (20 mg of eugenol was contained) were dissolved into ethanol (5 mL), respectively. The four groups of solution were then taken place



Scheme 1. The schematic diagram of the preparation of eugenol@MSNs.

into dialysis bags (M.W. 3500) and incubated in ethanol (50 mL) at 25 °C under horizontal shaking (150 rpm). At different time, solutions (0.5 mL) were removed and the same volume of fresh ethanol was added. The concentration of eugenol in the ethanol was measured by ultraviolet-visible spectrophotometer (UV-vis) at 278 nm wavelength. The release percentage of eugenol was calculated using formula (2):

$$\text{Released percentage (\%)} = W_1/W_2 \times 100\% \quad (2)$$

where W_1 is the weight of eugenol in the ethanol, W_2 is the weight of total eugenol in the nanoparticles.

All the data were analyzed in triplicate and presented as a mean value with standard deviation (mean \pm SD).

Mesoporous silica nanoparticles (MSNs) were prepared via sol-gel method. The morphology and size of MSNs were observed by TEM. As shown in Figs. 1A–C, all of them were spherical and the diameters were about 120 nm. Besides, all of the MSNs were uniformity and stability. These results indicated that the amount of *n*-hexane had almost no effect on the morphology and size of MSNs. The inner structures of MSNs were also observed by TEM (Figs. 1D–F). As shown in Fig. 1, there were obvious pore structures in MSNs. Besides, when the amount of *n*-hexane increased, the pore diameter of MSNs increased obviously. Therefore, *n*-hexane could significantly adjust the pore diameters of MSNs.

MSNs adsorbed fragrance molecules through mesoporous structure. Therefore, the performance of mesoporous structure is one of the most important characteristics of MSNs. The mesoporous structure of MSNs has been observed by TEM. The pore diameters, specific surface areas and pore volumes were measured by N_2 adsorption-desorption isotherm. As shown in Fig. 2A, the N_2 adsorption-desorption isotherms of all MSNs showed type IV isotherms. Compared with MSNs prepared by adding only 2 mL *n*-hexane, MSNs prepared by adding 25 mL and 30 mL *n*-hexane had large and obvious H2 hysteresis loop. Therefore, relatively large cage-type mesopores were formed when the amount of *n*-hexane was increased. The pore diameters of MSNs were then calculated. As shown in Fig. 2B, when the amount of *n*-hexane is 2 mL, 25 mL and 30 mL, the pore diameters of MSNs are 2.4 nm, 4.1 nm and 5.9 nm, respectively. The BET specific surface areas of MSNs with different pore diameters had similar specific surface areas, all of which were above 1300 m²/g (Fig. 2C). However, the pore volumes of MSNs with different pore diameters varied greatly. As shown in Fig. 2D, when large cage-type mesopores were formed, the pore volume of MSNs increased significantly, exceeding 2 cm³/g.

In the following, eugenol was encapsulated into MSNs and the fragrance-loaded nanoparticles were named eugenol@MSNs. The thermostability of eugenol@MSNs was detected by TGA. As shown in Figs. 3A–C, the free eugenol was almost completely decomposed at 160 °C. In contrast, eugenol encapsulated in MSNs could be completely decomposed at above 200 °C. This result indicated that the thermostability of MSNs encapsulated perfume was improved significantly. Moreover, the thermal stability of eugenol encapsulated in MSNs was better when the pore size decreased. The encapsulation efficiencies of eugenol were calculated by the TGA results. As shown in Fig. 3D, with the increase of pore sizes of MSNs, the encapsulation efficiency of eugenol increased significantly. Especially, when the pore diameter of MSNs was 5.9 nm, the encapsulation efficiency of eugenol reached 63.7%. The pore volume of MSNs with the pore diameter of 2.4 nm was smallest, so the encapsulation efficiency of eugenol@MSNs with the pore diameter of 2.4 nm was lowest. Interestingly, the pore volumes of MSNs with the pore diameter between 4.1 nm and 5.9 nm were closed, but the encapsulation efficiency of eugenol@MSNs with the pore diameter of 5.9 nm was significantly increased compared with

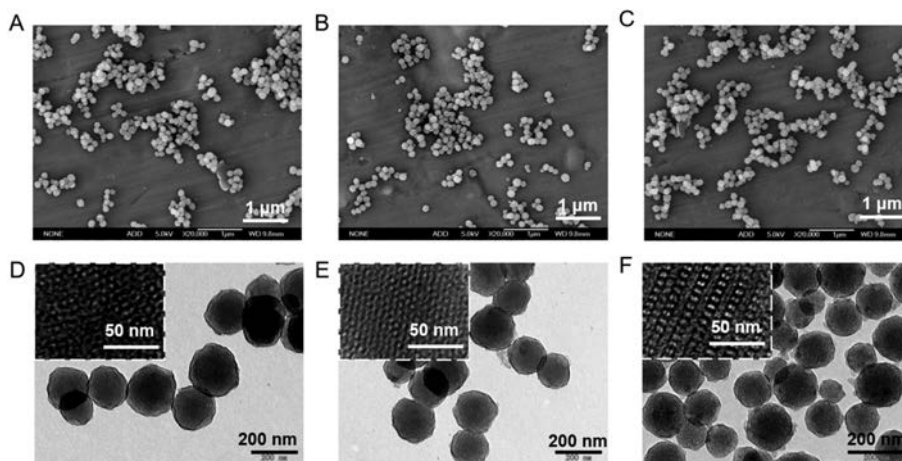


Fig. 1. The SEM images of MSNs obtained by sol-gel methods under the same conditions except that different amounts of *n*-hexane were used: (A, D) 2 mL, (B, E) 25 mL and (C, F) 30 mL. Scale bar: 1 μm (A–C), 200 nm (D–F).

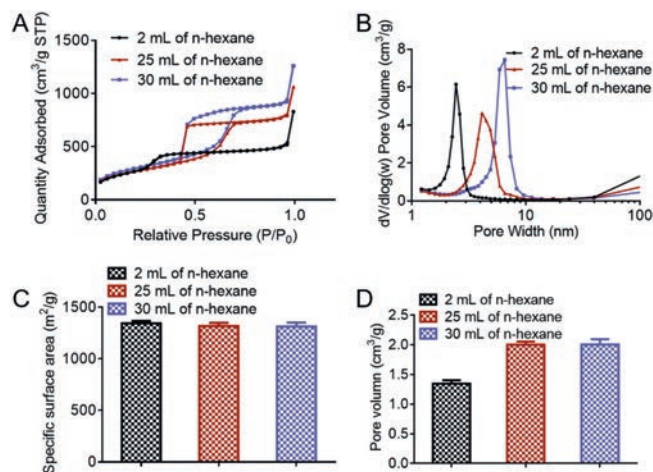


Fig. 2. (A) The N_2 adsorption-desorption isotherms at 77 K for MSNs. (B) The pore diameter distributions of MSNs. (C) The specific surface areas of MSNs. (D) The pore volumes of MSNs. The mean \pm SD is shown ($n = 3$).

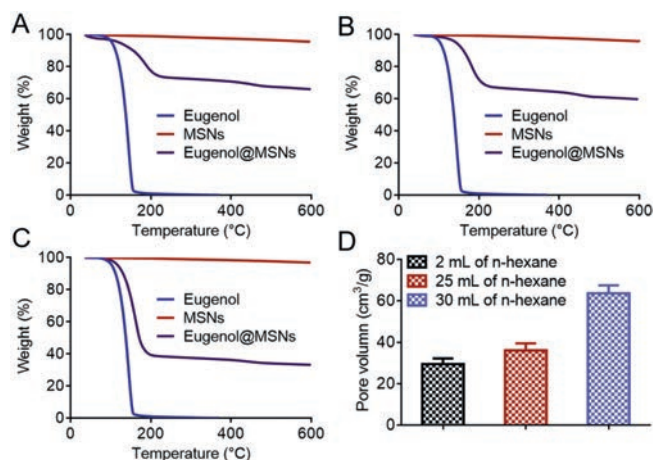


Fig. 3. (A–C) The TGA curves of eugenol, MSNs and eugenol@MSNs with different pore diameters: (A) 2.4 nm, (B) 4.1 nm and (C) 5.9 nm. (D) The encapsulation efficiencies of eugenol@MSNs with different pore diameters. The mean \pm SD is shown ($n = 3$).

that of eugenol@MSNs with the pore diameter of 4.1 nm. This might be due to the fact that when the pore diameters of MSNs increased, it was easier for fragrance molecules to enter the deep area of the long mesopores of MSNs.

Subsequently, the release profiles of eugenol were studied. As shown in Fig. 4, free eugenol was released rapidly. Nearly half of the free fragrance was released within 1 h. Almost all free eugenol was released within 2 h. In contrast, less than 35% of the fragrance was released from eugenol@MSNs with 72 h. These results proved that eugenol@MSNs could slow down the release rate of eugenol. The large specific surface areas of MSNs provided large adsorption capacity. The fragrance molecules were thus released slowly [32,33]. There was no significant difference in specific surface areas between the MSNs with pore diameters of 2.4 nm, 4.1 nm and 5.9 nm. However, there were obvious differences in release rates of eugenol between the MSNs with pore diameters of 2.4 nm, 4.1 nm and 5.9 nm. Therefore, the pore size also affected the release performance of the fragrance molecules. Eugenol@MSNs had the best sustained-release performance when the pore diameter of MSNs was 2.4 nm. Only 21.92% of eugenol was released from eugenol@MSNs within 72 h. However, when the pore size of MSNs was 4.1 nm and 5.9 nm, the sustained release performance of eugenol@MSNs was almost identical. This result indicated that the sustained release performance of eugenol@MSNs decreased with the increase of the pore size of MSNs. However, when the pore diameter of MSNs was larger than 4 nm, the pore size no longer affected the sustained-release performance of eugenol@MSNs.

Fragrances are involved in every aspect of our lives. The slow release of fragrances is very important for the application of fragrance products. Although there have been a lot of researches on sustained release of fragrances, most of them have not studied the cost of sustained release of fragrances and whether it can be produced in large scale. This is the key to transform from scientific

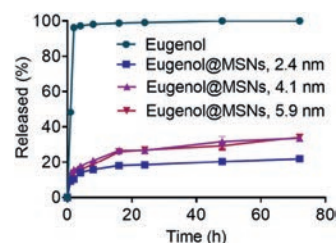


Fig. 4. The release profiles of free eugenol and eugenol@MSNs with different pore diameters. The mean \pm SD is shown ($n = 3$).

research to application. MSNs are low-cost nanomaterials that can be industrially produced in large scale. In addition, MSNs also have excellent stability. Therefore, the slow release of fragrances based on MSNs has a very good application prospect. However, for the loading and slow release of fragrances, most studies focus on surface modification, pore volume and specific surface area of MSNs. This makes it more difficult and expensive to prepare MSNs. In this study, the effects of pore diameters on the encapsulation and release of fragrances was explored. More importantly, the pore size could be adjusted by changing the amount of *n*-hexane, which hardly increased the cost and difficulty of MSNs. The larger the pore diameters of MSNs, the more fragrance molecules were absorbed and the release of eugenol was more rapid. But there was a little difference in the encapsulation efficiencies of eugenol@MSNs with the pore size between 2.4 nm and 4.1 nm. Besides, there was significant difference in the release rate of eugenol from eugenol@MSNs with the pore size between 4.1 nm and 5.9 nm. Therefore, encapsulating more fragrance molecule was more important, 5.9 nm was the most suitable pore diameter. If slow release of aromatic molecules was more important, 2.4 nm was the most suitable pore diameter.

In summary, MSNs with tunable pore size was prepared by adjusting the amount of *n*-hexane. With the increase of *n*-hexane, the pore size of MSNs increased significantly. All MSNs with different pore sizes had large specific surface area and pore volume. Especially, when the relatively large cage-type mesoporous were formed, the pore volume of MSNs increases obviously. Eugenol was then encapsulated into MSNs and the nano-fragrance was named eugenol@MSNs. The thermostability of eugenol encapsulated in MSNs was significantly improved. Besides, with the increase of pore size of MSNs, the encapsulation efficiency of eugenol increased significantly. Eugenol@MSNs had obvious sustained-release performance. In addition, with the decrease of pore size of MSNs, the sustained-release performance of Eugenol@MSNs was improved obviously.

Declaration of competing interest

The authors declare that they have no known competing financial interests or personal relationships that could have appeared to influence the work reported in this paper.

Acknowledgments

This work was financially supported by the National High Technology Research and Development Program (No. 2016YFA0200303), the Beijing Natural Science Foundation (Nos. L172046, 2192057), the National Natural Science Foundation of China (Nos. 31771095, 21875254 and 21905283).

References

- [1] G.Y. Zhu, Z.B. Xiao, R.J. Zhou, F.P. Yi, *Adv. Mater. Res.* 535–537 (2012) 440–445.
- [2] M.B. Pashazanousi, M. Raeesi, S. Shirali, *Asian J. Chem.* 24 (2012) 4331–4334.
- [3] S. Burt, *Int. J. Food Microbiol.* 94 (2004) 223–253.
- [4] M.G. Miguel, *Flavour Frag. J.* 25 (2010) 291–312.
- [5] J. Mastelic, I. Jerkovic, *Flavour Frag. J.* 18 (2003) 521–526.
- [6] L. He, J. Hu, W.J. Deng, *Polym. Chem.* 9 (2018) 4926–4946.
- [7] Z.B. Xiao, L. He, G.Y. Zhu, *Flavour Frag. J.* 29 (2014) 350–355.
- [8] D.L. Berthier, I. Schmidt, W. Fieber, et al., *Langmuir* 26 (2010) 7953–7961.
- [9] H. Yan, D. Zhu, Z. Zhou, et al., *Biomaterials* 178 (2018) 559–569.
- [10] Z. Guo, S. Li, Z.H. Liu, W. Xue, *ACS Biomater. Sci. Eng.* 4 (2018) 988–996.
- [11] J.W. Zhang, J.J. Cui, Y. Deng, Z.Z. Jiang, W.M. Saltzman, *ACS Biomater. Sci. Eng.* 2 (2016) 2080–2089.
- [12] Y.Y. Yuan, F.M. Gong, Y. Cao, et al., *J. Biomed. Nanotechnol.* 11 (2015) 668–679.
- [13] Q.Y. Meng, H. Hu, L.P. Zhou, et al., *Polym. Chem.* 10 (2019) 306–324.
- [14] X. Jia, M.L. Pei, X.B. Zhao, et al., *ACS Biomater. Sci. Eng.* 2 (2016) 1641–1648.
- [15] L.J. Song, A.Q. Zeng, M.X. Hu, et al., *J. Biomed. Nanotechnol.* 14 (2018) 267–280.
- [16] A. Gupta, S. Asthana, R. Konwar, M.K. Chourasia, *J. Biomed. Nanotechnol.* 9 (2013) 915–925.
- [17] Q. Zhou, S. Shao, J. Wang, et al., *Nat. Nanotechnol.* 14 (2019) 799–809.
- [18] J.Q. Wang, S.Q. Hu, W.W. Mao, et al., *Adv. Funct. Mater.* 29 (2019) 1807446.
- [19] Z.G. Lu, Y. Li, Y.J. Shi, et al., *Adv. Funct. Mater.* 27 (2017) 1703967.
- [20] H.L. Li, J.M. Li, X.Y. He, et al., *Chin. Chem. Lett.* 30 (2019) 1083–1088.
- [21] Q.Q. Hu, L. Bai, Z.J. Zhu, et al., *Chin. Chem. Lett.* 31 (2020) 915–918.
- [22] Z.G. Lu, J.Z. Wang, L.N. Qu, et al., *Bioact. Mater.* 5 (2020) 1127–1137.
- [23] Z.G. Lu, T.L. Zhang, J. Shen, et al., *J. Biomed. Nanotechnol.* 14 (2018) 1578–1589.
- [24] Z.G. Lu, T.L. Zhang, J. Yang, et al., *Eng. Life Sci.* 11 (2020) 535–540.
- [25] W.X. Gao, Y.L. Hu, L. Xu, et al., *Chin. Chem. Lett.* 29 (2018) 1795–1798.
- [26] L.P. Li, J. Song, J.G. Wang, W.B. Fan, *Mater. Express* 7 (2017) 283–290.
- [27] J.W. Wei, Y. Wang, J.X. Jiang, et al., *J. Biomed. Nanotechnol.* 15 (2019) 1097–1105.
- [28] K.H. Wu, Y.C. Chang, J.C. Wang, *Mater. Express* 9 (2019) 970–977.
- [29] N. Didry, L. Dubreuil, M. Pinkas, *Pharm. Acta Helv.* 69 (1994) 25–28.
- [30] D. Peixoto-Neves, J.H. Leal-Cardoso, J.H. Jaggat, *J. Cardiovasc. Pharmacol.* 64 (2014) 401–406.
- [31] J.Z. Wang, Z.G. Lu, J. Shen, et al., *J. Biomed. Nanotechnol.* 16 (2020) 652–658.
- [32] J. Shen, Z. Lu, T. Zhang, et al., *J. Biomed. Nanotechnol.* 14 (2018) 1556–1567.
- [33] W.H. Ji, T.L. Zhang, Z.G. Lu, et al., *Chin. Chem. Lett.* 30 (2019) 747–749.